



Calhoun: The NPS Institutional Archive
DSpace Repository

Reports and Technical Reports

All Technical Reports Collection

2022-04

Conceptual Design of an Open-Source Hardware Simplified Floating Spacecraft Simulator

Kulke, Josef

Monterey, California. Naval Postgraduate School

<http://hdl.handle.net/10945/69412>

This publication is a work of the U.S. Government as defined in Title 17, United States Code, Section 101. Copyright protection is not available for this work in the United States.

Downloaded from NPS Archive: Calhoun



Calhoun is the Naval Postgraduate School's public access digital repository for research materials and institutional publications created by the NPS community. Calhoun is named for Professor of Mathematics Guy K. Calhoun, NPS's first appointed -- and published -- scholarly author.

Dudley Knox Library / Naval Postgraduate School
411 Dyer Road / 1 University Circle
Monterey, California USA 93943

<http://www.nps.edu/library>

NPS-SP-22-001



**NAVAL
POSTGRADUATE
SCHOOL**

MONTEREY, CALIFORNIA

CONCEPTUAL DESIGN OF AN OPEN-SOURCE HARDWARE

SIMPLIFIED FLOATING SPACECRAFT SIMULATOR

by

Josef Kulke

April 2022

Distribution Statement A

Approved for public release; distribution is unlimited

Prepared for: Universität der Bundeswehr Hamburg

THIS PAGE INTENTIONALLY LEFT BLANK

REPORT DOCUMENTATION PAGE

PLEASE DO NOT RETURN YOUR FORM TO THE ABOVE ORGANIZATION.

1. REPORT DATE 04/05/2022	2. REPORT TYPE Technical Report	3. DATES COVERED	
		START DATE 02/14/2022	END DATE 03/30/2022
4. TITLE AND SUBTITLE Conceptual Design of an Open-Source Hardware Simplified Floating Spacecraft Simulator			
5a. CONTRACT NUMBER	5b. GRANT NUMBER	5c. PROGRAM ELEMENT NUMBER	
5d. PROJECT NUMBER	5e. TASK NUMBER	5f. WORK UNIT NUMBER	
6. AUTHOR(S) 2 nd Lt, Josef Kulke, B.Sc., German Air Force			
7. PERFORMING ORGANIZATION NAME(S) AND ADDRESS(ES) Spacecraft Robotics Laboratory Department for Mechanical and Aerospace Engineering Naval Postgraduate School Monterey, CA, 93943			8. PERFORMING ORGANIZATION REPORT NUMBER NPS-SP-22-001
9. SPONSORING/MONITORING AGENCY NAME(S) AND ADDRESS(ES) Universität der Bundeswehr Hamburg Fakultät für Maschinenbau Professur für Mechatronik Holstenhofweg 85 22043 Hamburg, Germany		10. SPONSOR/MONITOR'S ACRONYM(S) UniBw H, HSU	11. SPONSOR/MONITOR'S REPORT NUMBER(S)
12. DISTRIBUTION/AVAILABILITY STATEMENT Distribution Statement A: Approved for public release; distribution is unlimited			
13. SUPPLEMENTARY NOTES Thesis Examiners: Univ.-Prof. Dr.-Ing. Delf Sachau (HSU), Prof. Dr. Marcello Romano (NPS)			
14. ABSTRACT This thesis covers parts of the development of a new open-source hardware Floating Spacecraft Simulator for teaching and research purposes, named MyDAS, standing for Mini Dynamic Autonomous Spacecraft Simulator. A Floating Spacecraft Simulator (FSS) is an autonomous robotic vehicle which floats via air bearings on a smooth surface, is actuated by thrusters and controlled by an on-board computer. The use of FSS is advantageous as a cost-effective ground-test tool providing a level of fidelity between numerical simulations and orbital flight. Research has shown that physical validation is important for advancing autonomous spacecraft maneuvers. Even though many FSS are in use worldwide in universities, research centers and industries, they are typically custom developed and expensive items. In this thesis for the first time, to the best knowledge of the author, a FSS is introduced which is designed to be as small and as inexpensive as possible, while maintaining a high level of spacecraft-emulation fidelity. By introducing MyDAS, the author aims at a broader utilization of spacecraft simulators for research and education at university level, and possibly also high-school level. In addition to being small and inexpensive, MyDAS shall use off-the-shelf and 3D-printed components to allow for customization and improvement. The preliminary design of MyDAS addresses three primary systems necessary to develop a miniature, simplified FSS. These systems include pneumatics, electronics, and structure. The fundamentals, the state of the art, as well as the conceptual design of this specific FSS are presented in this thesis.			
15. SUBJECT TERMS Open-Source, Open-Source Hardware, FSS, Floating Spacecraft Simulator, inexpensive, simple, simplified, modular, standardized			
16. SECURITY CLASSIFICATION OF:			17. LIMITATION OF ABSTRACT
a. REPORT unclassified	b. ABSTRACT unclassified	c. THIS PAGE unclassified	unclassified
			18. NUMBER OF PAGES 54
19a. NAME OF RESPONSIBLE PERSON Josef Kulke			19b. PHONE NUMBER (Include area code)

THIS PAGE INTENTIONALLY LEFT BLANK

**NAVAL POSTGRADUATE SCHOOL
Monterey, California 93943-5000**

Ann E. Rondeau
President

Scott Gartner
Provost

The report entitled “Conceptual Design of an Open-Source Hardware Simplified Floating Spacecraft Simulator” was prepared for “Universität der Bundeswehr Hamburg” and funded by “German Armed Forces”.

Distribution Statement A: Further distribution of all or part of this report is authorized.

This report was prepared by:

2nd Lieutenant Josef Kulke, German Air Force
B.Sc.

Reviewed by:

Released by:

James Newman, Chairman
Space Systems Academics Group

Kevin B. Smith
Dean of Research

THIS PAGE INTENTIONALLY LEFT BLANK



HELMUT SCHMIDT
UNIVERSITÄT

Universität der Bundeswehr Hamburg

Studienarbeit

Conceptual Design of an Open-Source Hardware Simplified Floating Spacecraft Simulator

Josef Kulke

März 2022

Studienarbeit zum Thema: Floating Spacecraft Simulator

Conceptual Design of an Open-Source Hardware
Simplified Floating Spacecraft Simulator

Abgabe: 30.03.2022

Josef Kulke
Matrikelnummer 00893450
Maschinenbau
St.-Jahrgang 2018

Erstgutachter: Univ.-Prof. Dr.-Ing. Delf Sachau (HSU)
Zweitgutachter: Professor Dr. Marcello Romano (NPS)

Professur Mechatronik
Fakultät Maschinenbau
Helmut-Schmidt-Universität / Universität der Bundeswehr Hamburg

Spacecraft Robotics Laboratory
Department of Mechanical and Aerospace Engineering
Naval Postgraduate School


Hamburg, 2022

Declaration of Authorship

I hereby declare that this thesis and the work presented in it is entirely my own. All direct or indirect sources used are acknowledged as references.

Erklärung selbstständiger Bearbeitung

Hiermit versichere ich, dass ich die vorliegende Abschlussarbeit selbstständig und ohne fremde Hilfe verfasst habe. Insbesondere versichere ich, dass ich alle wörtlichen und sinngemäßen Übernahmen aus anderen Werken als solche kenntlich gemacht habe.

Monterey, 30.03.2022 

Place, Date, Signature

Acknowledgments

The work presented in this thesis was assisted and made possible by several people, whose actions are greatly appreciated.

First and foremost, the author would like to thank Dr. Stephen Kwok-Choon for his expertise in all belongings regarding this thesis. He helped at all times with all problems.

Furthermore, Dr. Bautista Fernandez was always there to give precious technical advice, in addition to placing the orders for the components.

Moreover, the author is grateful for the supervision of Professor Marcello, who had the idea and several design proposals for this project in the first place.

Last but not least, the research stay abroad for this thesis was made possible by Professor Delf Sachau from Helmut-Schmidt-University/University of the Federal Armed Forces Hamburg.

Abstract

This thesis covers parts of the development of a new open-source hardware Floating Spacecraft Simulator for teaching and research purposes, named MyDAS, standing for Mini Dynamic Autonomous Spacecraft Simulator. A Floating Spacecraft Simulator (FSS) is an autonomous robotic vehicle which floats via air bearings on a smooth surface, is actuated by thrusters and controlled by an on-board computer. The use of FSS is advantageous as a cost effective ground-test tool providing a level of fidelity between numerical simulations and orbital flight. Research has shown that physical validation is important for advancing autonomous spacecraft maneuvers. Even though many FSS are in use worldwide in universities, research centers and industries, they are typically custom developed and expensive items. In this thesis for the first time, to the best knowledge of the author, a FSS is introduced which is designed to be as small and as inexpensive as possible, while maintaining a high level of spacecraft-emulation fidelity. By introducing MyDAS, the author aims at a broader utilization of spacecraft simulators for research and education at university level, and possibly also high-school level. In addition to being small and inexpensive, MyDAS shall use off-the-shelf and 3D-printed components to allow for customization and improvement. The preliminary design of MyDAS addresses three primary systems necessary to develop a miniature, simplified FSS. These systems include pneumatics, electronics and structure. The fundamentals, the state of the art, as well as the conceptual design of this specific Floating Spacecraft Simulator are presented in this thesis.

Contents

List of Figures	viii
List of Tables	ix
List of Acronyms	x
Nomenclature	xi
1 Introduction	1
1.1 Motivation	1
1.2 Objective	1
1.3 Structure	2
2 Fundamentals	3
2.1 Air Bearings	3
2.2 Propulsion	5
3 State of the Art	6
3.1 Floating Spacecraft Simulators in General	6
3.2 FSS at Naval Postgraduate School	8
4 Equations of Motion	10
4.1 Assumptions	10
4.2 General Equations	10
4.3 Simplified Equations	11
4.4 Propulsion Configurations	13
5 Pneumatics	15
5.1 Compressed Air Supply	15
5.2 Air Bearings	17
5.3 Floating Duration	19
5.4 Thrusters	21

6	Electronics	22
6.1	Power Supply and Distribution	22
6.2	Electronic Parts	24
7	Design Work	26
7.1	3D Sketching	26
7.2	Conceptual Parametric Modeling	27
7.3	Conceptual Assembly	29
8	Conclusions	30
8.1	Summary	30
8.2	Future Work	31
	References	I
	Appendix	IV

List of Figures

2.1	Working principle of an air bearing [5].	3
2.2	A comparison of friction coefficients between plain-, rolling- and air bearings [5].	4
3.1	Jet Propulsion Laboratory (JPL)'s Formation Control Testbed [9].	6
3.2	The chaser and target vehicle of Univerity of Rome's testbed [14].	7
3.3	All four FSS generations built at the Spacecraft Robotics Laboratory (SRL) from left to right [15].	8
4.1	Rigid body with forces and a moment in an inertial reference frame.	11
4.2	The meaning of r in the context of the equations of motion.	12
4.3	A schematic depiction of all three propulsion configurations in question.	13
5.1	A schematic diagram showing the airflow for the pneumatics of MyDAS.	16
5.2	A technical drawing of an 80 mm flat round air bearing [22].	17
5.3	Lift versus load curve for the 25 mm flat round air bearing [23].	18
5.4	Laval nozzle used for MyDAS, mounted onto the solenoid valve.	21
6.1	A schematic diagram of the wiring for MyDAS.	23
6.2	An exemplary setup for the VIVE tracking system.	25
7.1	A render of the most important components in place, but without a frame.	27
7.2	Illustration of the bottle container and the platform.	28
7.3	Illustration of thruster and servo mounting rings.	28
7.4	Assembly of some components for two variants of MyDAS.	29

List of Tables

5.1	The final three air tanks for consideration [19], [20], [21].	15
5.2	Air bearings of different diameters with their corresponding ideal load [24].	19
5.3	Values for determination of mass of air inside air tank.	19
5.4	Air flow and floating time for each air bearing under no load at 4.1 bar.	20
8.1	Complete parts list for the pneumatics, including different options.	IV
8.2	Complete parts list for basic assembly items, including different options.	V
8.3	Complete parts list for the electronics, including different options.	VI

List of Acronyms

BoM	Bill of Materials
CGP	Cold gas Propulsion
CMG	Control Moment Gyroscope
DoF	Degrees-of-Freedom
FSS	Floating Spacecraft Simulator
FCT	Formation Control Testbed
GNC	Guidance, Navigation and Control
IMU	Inertial Measurement Unit
JPL	Jet Propulsion Laboratory
MOPD	Maximum Operating Pressure Difference
MyDAS	Mini Dynamic Autonomous Spacecraft Simulator
NPS	Naval Postgraduate School
RW	Reaction Wheel
SCFH	Standard Cubic Feet per Hour
SRL	Spacecraft Robotics Laboratory
SSDT	Small Satellite Dynamics Testbed

Nomenclature

\varnothing	diameter
\vec{a}	$[3 \times 1]$ linear acceleration vector of center of mass
A_e	cross-sectional area of nozzle exit
$\ddot{\vec{\varphi}}$	$[3 \times 1]$ angular acceleration vector
$\ddot{\varphi}$	angular acceleration about z -axis
\vec{e}_z	unit vector in z -direction
\vec{F}	$[3 \times 1]$ force acting on FSS
F	absolute value of force vector \vec{F} , disregarding z -component
\vec{J}	$[3 \times 3]$ moment of inertia matrix about center of mass
J	moment of inertia about z -axis through center of mass
\vec{l}	$[3 \times 1]$ leverage of force vectors
m	total mass of FSS
m_{air}	mass of air inside air tank
\dot{m}	mass flow of exiting air
\vec{M}	$[3 \times 1]$ moment acting on FSS
p	variable that adds or subtracts moments
P_e	pressure at nozzle exit
P_a	ambient pressure
r	projected shortest distance from force line to center of mass
$\rho_{\text{air,high}}$	air density at 207 bar (3000 psi)
$\rho_{\text{air,low}}$	air density at atmospheric pressure
τ	thrust
ϑ_{air}	temperature of air inside air tank
v_e	exit velocity
V_{airtank}	volume of air tank

1 Introduction

The motivation for the research, the objective of the author's work and the structure of this document are explained in this chapter.

1.1 Motivation

Future space missions require flexible autonomous Guidance, Navigation and Control (GNC) systems, for example for autonomous docking, proximity and debris removal maneuvers [1], [2], [3]. One way to experimentally test GNC algorithms with hardware-in-the-loop, but without sending test subjects to space, is to use Floating Spacecraft Simulators (FSS). By creating a thin film of air between the FSS and a smooth surface, the FSS floats above the surface and therefore it has almost no friction. This technique allows to simulate certain Degrees-of-Freedom (DoF) and copy conditions that real satellites are exposed to. However, such spacecraft simulators are mostly unique builds that are expensive and relatively large. To this date, conducting tests with FSS requires a lot of economical and time-consuming effort, which is only possible for dedicated institutions or companies. Bringing the possibility to work on FSS to the broad public could ease the process of developing GNC algorithms for spacecraft, resulting in more successful and advanced space missions in the future.

1.2 Objective

This thesis shall present the concept of a simpler, smaller, and affordable FSS in comparison to the ones already in existence. The device shall be reproducible, meaning that the components are either obtainable off-the-shelf or can be manufactured with low cost and effort, e.g. 3D-printed. It will be named MyDAS, standing for Mini Dynamic Autonomous Spacecraft Simulator. For that purpose, older FSS are compared and the theory behind FSS is taken into account. The final device must be able to float and propel itself using its own compressed gas supply. Furthermore, the propulsion system must be controlled by an on-board computer which is powered by its own battery system. If possible, the duration for the floatation shall exceed five minutes without using air for the propulsion system. The goal of this thesis is to have a bill of materials, a pneumatic systems diagram, a wiring schematic and 3D sketches for the new spacecraft simulator MyDAS. MyDAS is to be physically assembled and experimentally tested in future work.

1.3 Structure

To understand the working principles of FSS, chapter 2 *Fundamentals* is designated to explaining these. In that chapter, a rough overview of satellite maneuvering, air bearings and cold gas thrusters is given. Additionally, different propulsion configurations are proposed. In chapter 3 *State of the Art*, past and current FSS are examined and compared. This helps to understand where and why major design changes for MyDAS in comparison to older designs are necessary. Some simplified equations of motion are introduced in chapter 4 *Equations of Motion*. Chapter 5 *Pneumatics* discusses the pneumatic system as planned for MyDAS, while chapter chapter 6 *Electronics* treats the electrical components. The construction of a custom, 3D-printed housing which holds all components in place is the main subject of chapter 7 *Design Work*. The last chapter, named *Conclusions*, gives a summary of the work, as well as recommendations for future work.

2 Fundamentals

The main property encountered by satellites in space which is difficult to replicate on earth is weightlessness. This means that no force that is acting on an observer can be felt and the observer is freely floating. A free floating rigid body in space has six Degrees-of-Freedom, three rotational and three translational ones. To replicate the full motion spectrum for a physical simulator, all six DoF would have to be considered. However, FSS with only one floating surface cannot simulate all six DoF due to their working principles. This is not always necessary though, as GNC systems can be tested on a platform with less DoF [4]. MyDAS is designed to float on a flat and level test bed, which provides two translational and one rotational DoF.

2.1 Air Bearings

The air bearing receives pressurized air from a compressed air tank. It then distributes the air so that it leaves the air bearing evenly through a porous surface [5]. When the bottom face of the air bearing is placed on a smooth surface that matches the geometry of the face of the air bearing, a thin film of pressurized air makes the air bearing hover over the surface in the order of tens to hundreds of microns. In the case of MyDAS, as described above, the guiding surface is flat and even. Therefore, flat air bearings have to be used. The guiding surface must be well aligned horizontally, as just little slope creates an unwanted artificial gravity effect which would cause the FSS to slide off the table. Figure 2.1 shows the working principle of an air bearing.

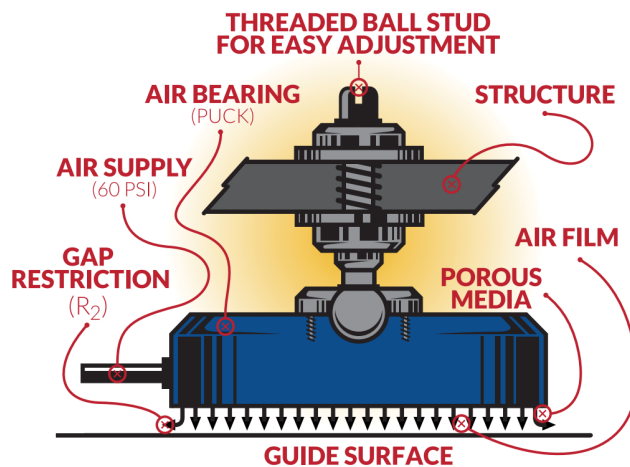


Figure 2.1: Working principle of an air bearing [5].

Theoretically, the DoF could be realized using linear rolling bearings for the translation and round rolling bearings for the rotation. The key factor why MyDAS uses air bearings and they have been used previously is the low friction coefficient of the bearing. Air bearings have a friction coefficient that is several orders of magnitude smaller than that of any rolling bearing. Figure 2.2 shows a comparison in friction coefficients between air bearings, rolling bearings and plain bearings.

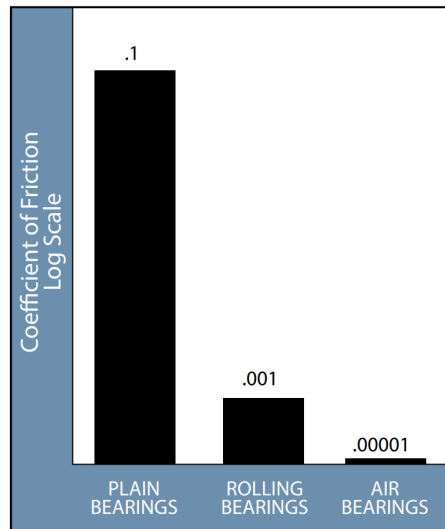


Figure 2.2: A comparison of friction coefficients between plain-, rolling- and air bearings [5].

2.2 Propulsion

Small satellites are launched to space in larger spacecraft which then separate. For launch and getting into orbit, the carrying spacecraft provides thrust, but after separation, the satellite is on its own. To correct its position in orbit, dock to other objects in space, or generally serve their purpose, satellites must have an own propulsion system. While there are numerous ways to create forces and moments to accelerate spacecraft, most of them can be classified into two categories: Ones that actively use power to propel, and ones that only use power to initiate and terminate the propulsion [6]. MyDAS, as well as all previous generations of FSS at Spacecraft Robotics Laboratory (SRL), uses the latter for different reasons. Pricing and simplicity are two of them. Specifically, the principle of Cold gas Propulsion (CGP) is used.

Compressed gas stored inside the spacecraft exits via a laval-nozzle. If the pressure ratio of the pressure before the nozzle and after the exit is high enough, the gas will reach sonic speed at the narrowest section. After that, it expands and accelerates to super sonic speed. The momentum created by the acceleration of the mass creates a corresponding reaction force, pushing the nozzle, and hence the spacecraft, in the opposite direction. This is based on Newton's third law. In addition to the thrust based on the acceleration, a certain amount of thrust is added by the pressure at the exit of the nozzle, compared to ambient pressure. Summed up, the equation for the thrust generated is [6]:

$$\tau = \dot{m}v_e + (P_e - P_a)A_e \quad (2.1)$$

The symbol τ denotes the thrust, while \dot{m} stand for the mass flow of gas exiting, v_e stands for the exit velocity of the gas, P_e is the ambient pressure, P_a is the exit pressure of the gas and A_e is the exit area of the nozzle. Thrust can be increased by increasing the pressure at which the gas enters the nozzle. This goes in a proportionate manner, as [6] describes. In [7], experiments were done for CGP systems in the order of magnitude of 0.1 N. The results show a slightly lower than linear correlation of pressure versus thrust, i.e. doubling the input pressure multiplies the thrust by little less than two. Different gases are possible to use, two common ones are CO₂ and air.

For attitude control, central elements of any spacecraft are Reaction Wheels (RWs) and Control Moment Gyroscopes (CMGs). They can only control the attitude of a spacecraft, while the thrusters can control the attitude and location. However, it was decided to leave RWs and CMGs out of MyDAS due to cost and complexity factors. Therefore, these systems are not further explained in this thesis.

3 State of the Art

This chapter serves to give an overview of what has been done in the field of FSS. Floating Spacecraft Simulators have been around for almost 65 years, and their development began parallel with the development of real spacecraft [8]. Several historical reviews had already been conducted.

3.1 Floating Spacecraft Simulators in General

NASA’s Jet Propulsion Laboratory (JPL) has multiple FSS test beds. One of them is a six DoF flat testbed for formation maneuvering with two FSS. It is called the Formation Control Testbed (FCT). The DoF in the horizontal plane are realized with flat air bearings floating over the floor. The rotational DoF are realized with a spherical air bearing mounted on the top of a vertical stage, giving it the third translational DoF [9]. The dimensions of the FCT are relatively large, as it is about 1.27 m wide [9] and weighs around 100 kg [10]. Figure depicts 3.1 the FCT testbed.

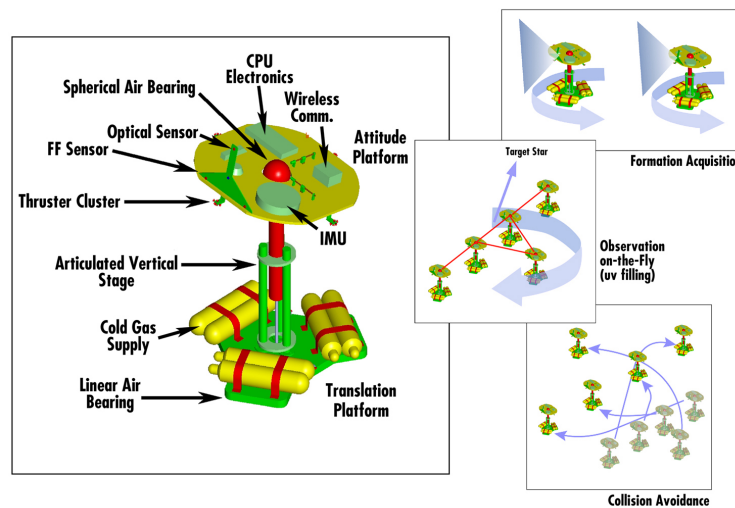


Figure 3.1: JPL’s Formation Control Testbed [9].

Another testbed by NASA’s JPL is the Small Satellite Dynamics Testbed (SSDT). It is smaller than the FCT and only has three DoF, but is made for smaller satellites. The platform is propelled by eight compressed air thrusters operating at 6.2 bar and uses planar air bearings at the same pressure. The pressure for the thrusters and the air bearings is regulated separately. Each

thruster produces approximately 0.5 N of thrust, with multiple thrusters firing simultaneously creating slightly less individual thrust. It weighs around 30 kg and is roughly 0.5 m wide [10]. Several characterizations of this FSS were done, which are also due for MyDAS in future work.

Kwok-Choon et al. presented the design of a 30 cm x 30 cm planar FSS with eight thrusters and a total mass of approximately 15 kg. Each of the eight thrusters generated between 0.3 N and 0.4 N of thrust. As an on-board computer, two Arduinos were used [11].

Polish researchers introduced a new planar microgravity simulator which consists of a base and a manipulator arm with two joints. The base floats on three air bearings and the manipulator arm on two further air bearings. Planar translation and rotation about the vertical axis, plus one DoF for each joint gives the total of five DoF. The mass of the base is around 13 kg and combined with the arm it weighs almost 19 kg [12].

Researchers from the University of Rome La Sapienza built the PINOCCHIO FSS planar testbed. Two FSS simulate a satellite chasing a target in space. The chaser vehicle has a mass of 8.7 kg and dimensions of 20 cm x 20 cm x 45 cm. It has separate sets of thrusters for attitude and location control. Four thrusters, each at an angle of 90° to each other pointing through the center of mass are responsible for the translation. For the rotation, a parallel configuration, as explained in section 4.4, is used. Therefore, a total of twelve thrusters are on board the chaser vehicle. The target vehicle propels itself using computer fans [13], [14]. Figure 3.2 shows an image of the chaser and target vehicle.

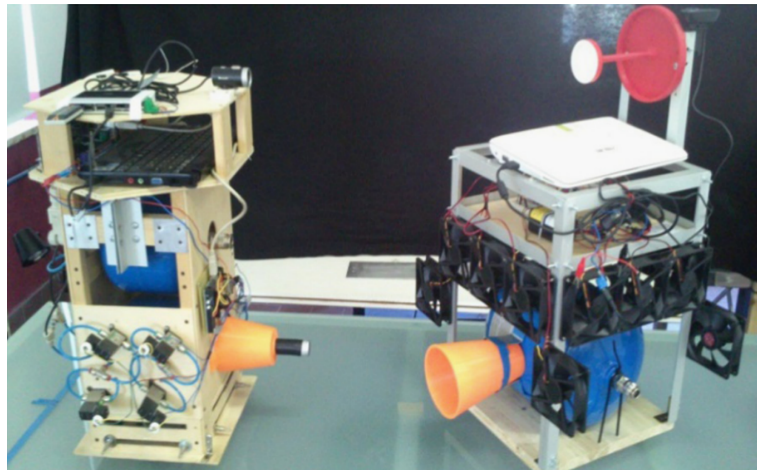


Figure 3.2: The chaser and target vehicle of University of Rome's testbed [14].

3.2 FSS at Naval Postgraduate School

The main inspiration for the design of MyDAS comes from older FSS built by the SRL at Naval Postgraduate School (NPS). There were four generations of planar FSS constructed at SRL. All of them had planar translation and rotation about the vertical axis. Some of them additionally had manipulator arms, giving them in total more than three DoF. Most of them used three to four 25 mm flat round air bearings to support the structure, since the footprint of the overall structure is much larger than the surface of a single air bearing. The propulsion system was different for each generation. They all used compressed air thrusters with different numbers and arrangements. Some of them, however, had RWs with them, others even had a CMG, or both. To decrease the weight, the third and fourth generation used 3D-printed polycarbonate structures [15]. Reference [16] describes the hardware of the second generation. It weighs approximately 26 kg and its dimensions are 30 cm x 30 cm x 69 cm. As for the propulsion systems, it has a CMG and two vectorable thrusters with 0.16 N of thrust each. Its continuous operation time is limited by the air supply and is around 40 min. Even without the CMG, this configuration is controllable by the Small Time Local Controllability definition [4]. Reference [15] explains the physical properties of the fourth generation. With less than 10 kg and a size of 27 cm x 27 cm x 52 cm it is a little bit smaller, but much lighter compared to the second generation. It has eight thrusters with 0.1 N - 0.15 N thrust each, and a reaction wheel with 2.5 Nms of angular momentum. In order to track its location, small passive markers are mounted on the FSS, while several fixed cameras from the outside capture these dots. In a software, by analyzing the different viewpoints, the location and attitude can be determined. Figure 3.3 depicts all four generations.

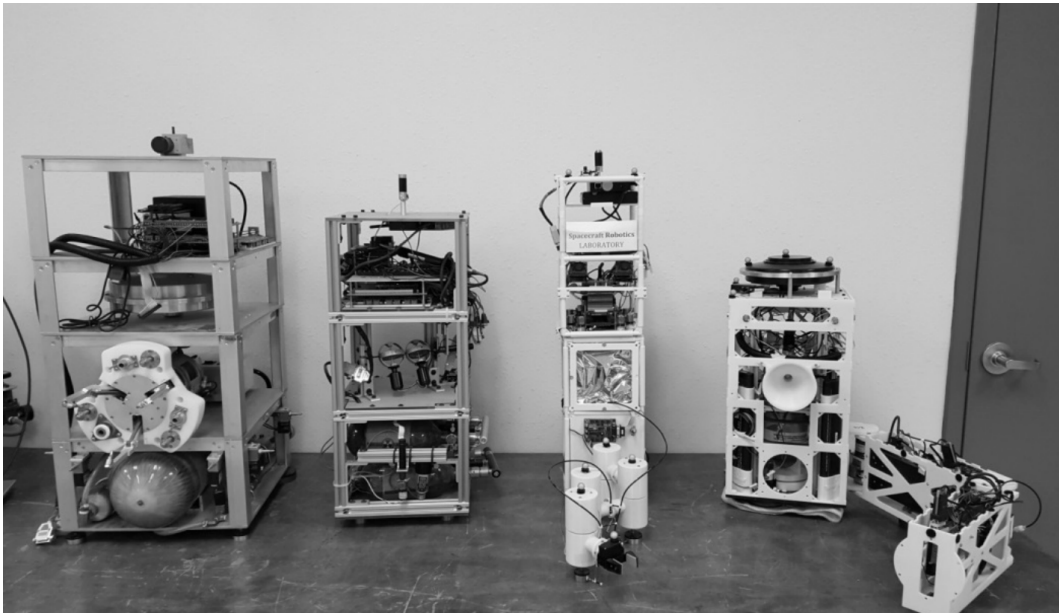


Figure 3.3: All four FSS generations built at the SRL from left to right [15].

From the cited references, it emerges that no Floating Spacecraft Simulator in a hand-portable size has been created. Furthermore, all designs differ strongly and show a lot of room for improvement regarding standardization and simplification. A multitude of different propulsion mechanisms was used, some of which are considered for MyDAS. Further reviews and analyses regarding the state of the art for FSS testbeds can be found in [8], [10], [17], [18].

4 Equations of Motion

Constructing a Floating Spacecraft Simulator requires the designer to give thoughts about the equations of motion, since the designer has to set up a propulsion system, which strongly influences these equations. The equations are necessary to later implement the GNC algorithms which the FSS has to experimentally validate.

4.1 Assumptions

Simulating the environment of a satellite in space and limiting the DoF to three makes the dynamics of a rigid body relatively simple to describe. The order of magnitude for the speed achieved with this FSS is of cm/s, which, combined with the relatively small cross section, results in negligible air resistance. Friction coming from the air bearing, as shown in chapter 2 is also neglected. Gravitational forces, for instance from an uneven floating surface, are also disregarded. For that reason, this thesis assumes free translational movement along the horizontal plane (x - y -plane) and free rotational movement along the vertical axis (z -axis). The mass of the FSS is assumed to be constant, because the loss of air due to the air bearings and thrusters firing is estimated to be in the order of only 1 % of the total mass.

4.2 General Equations

By regarding a rigid body in an inertial frame of reference, two general equations for the motion of the body can be set.

$$m\vec{a} = \sum_i \vec{F}_i \quad (4.1)$$

$$\vec{J}\ddot{\vec{\varphi}} = \sum_i \vec{l}_i \times \vec{F}_i + \sum_j \vec{M}_j \quad (4.2)$$

The letter m is the total mass of the body and \vec{J} is the $[3 \times 3]$ moment of inertia matrix with respect to the center of mass. \vec{F}_i are force vectors and \vec{M}_k are direct moments that act on the body, causing linear and angular acceleration. The vector \vec{a} is the linear acceleration of the center of mass, and the vector $\ddot{\vec{\varphi}}$ represents the angular acceleration about the center of mass.

Moments can either be directly applied, e.g. by a RW, or indirectly through a force that is not pointing through the center of mass, giving it a leverage. The leverage \vec{l}_i is described as a vector from the center of mass to the point at which the force acts. Figure 4.1 shows a schematic representation of a rigid body in the coordinate system with forces and a moment acting on it.

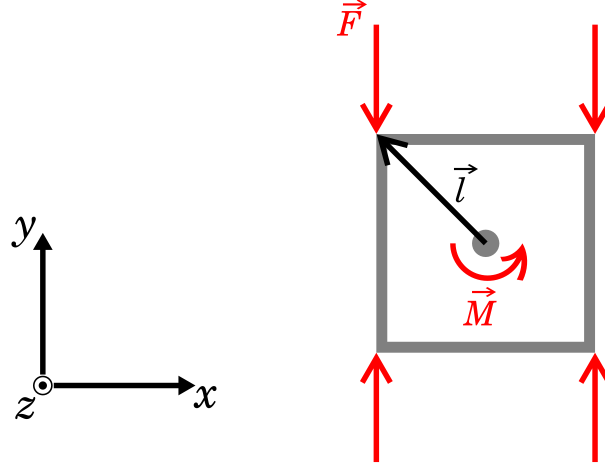


Figure 4.1: Rigid body with forces and a moment in an inertial reference frame.

4.3 Simplified Equations

Adapting these equations for MyDAS results in zero linear acceleration in z -axis, and angular acceleration only about the z -axis, given by the DoF. Therefore, all corresponding components have to be restricted and will be set to zero:

$$a_z = 0 \quad (4.3)$$

$$F_{i,z} = 0, \forall i \quad (4.4)$$

The moment of inertia does not need a matrix anymore and henceforth the letter J will be used for the moment of inertia about the z -axis through the center of mass, while $\ddot{\varphi}$ describes the angular acceleration about the z -axis. The unit vector \vec{e}_z extracts the z -component out of the cross product, as it is the only non-zero component. Since MyDAS does not include a RW or CMG, direct moments \vec{M}_j can be excluded from equation 4.2. Then, equation 4.2 can be simplified to:

$$J\ddot{\varphi} = \sum_i (\vec{l}_i \times \vec{F}_i) \cdot \vec{e}_z \quad (4.5)$$

In order to simplify equation 4.5 even more, forces are regarded only by their absolute value $|\vec{F}|$, which is newly defined as F . Leverage vectors \vec{l} are replaced with r , the shortest distance from the center of mass to the line on which each force acts, projected onto the x - y -plane. The purely scalar equation for the angular acceleration turns out to be:

$$J\ddot{\phi} = \sum_i p_i r_i F_i \quad (4.6)$$

It is important to note that F and r are physical properties and are therefore greater than or equal to zero. Since forces can also create a negative moment, the variable p takes accounts for that, by defining it to be -1 if the force F creates a negative moment and +1 if otherwise. In the case of Figure 4.2, F_2 creates a positive moment, based on the coordinate system shown in Figure 4.1. Therefore, p_2 counts positive and p_1 negative, since F_1 creates a moment in the opposite direction. Figure 4.2 shows a graphical illustration for r .

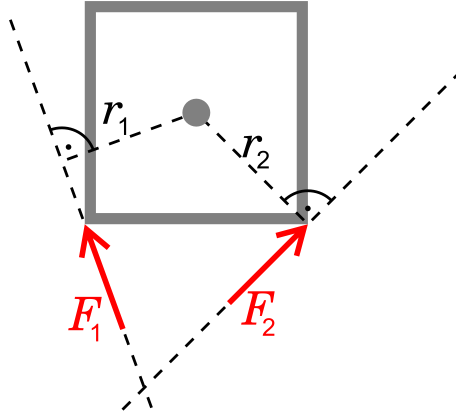


Figure 4.2: The meaning of r in the context of the equations of motion.

The idea from here on is to assign a force vector for each thruster and specify the values of r_i and F_i . With equations 4.1 and 4.6, while holding on to the constraints of equations 4.3 and 4.4, the dynamics of MyDAS can be described. The reason for keeping these equations so general is that three different propulsion configurations are under consideration. In order not to go beyond the scope of this thesis, none of them are further examined. In future work, the final propulsion configuration will then be analyzed.

4.4 Propulsion Configurations

All three configurations use only thrusters, but no RW or CMG, as stated and justified above. Two of the three configurations use four fixed thrusters, while one configuration uses only two, but vectorable thrusters. The vectoring will be realised by mounting each thruster onto a 180° servo motor. Figure 4.3 shows the three configurations schematically. Depicted is the body of the FSS with its center of mass in grey, and a red force vector for each thruster with location and orientation.

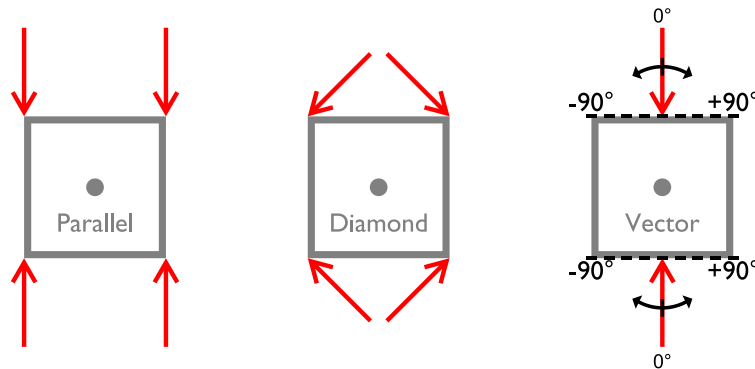


Figure 4.3: A schematic depiction of all three propulsion configurations in question.

4.4.1 Parallel Configuration

The configuration shown on the left, with four parallel thrusters, was chosen because it gives direct motion control in two directions (up and down). To do that, two thrusters which face in the same direction must fire simultaneously. For rotating the spacecraft, two diagonally opposite thrusters must fire. If the center of mass is balanced, either of those operations will only translate, respectively rotate the FSS without doing the other. To move the FSS sideways, it has to rotate first, and then move in its forward or backwards direction. This brings the main disadvantage that no direct sideways motion can be realized.

4.4.2 Diamond Configuration

This is different for the diamond configuration, shown in the middle. It is possible to accelerate the FSS in four local directions at any point in time. For that, two thrusters on the same side must fire simultaneously. To rotate, just like with the parallel configuration, two thrusters on the opposite side must fire at the same time. One downside of this configuration is that for linear motion, the lateral parts of the thrust vectors cancel out and are hence wasted. As all the thrusters are orientated 90° to each other and 45° to the main directions, an efficiency of $\frac{\sqrt{2}}{2} \approx 70.7\%$ is inherently given.

4.4.3 Vector Configuration

The last configuration only uses two, but vectorable thrusters. They are placed opposite of each other with respect to the center of mass. When the servos are at their default positions at 0° , both thrusters face out to the side, in opposite directions. By firing one of them, linear acceleration in the corresponding direction is achieved. To move sideways, both servos have to rotate in the same direction to $\pm 90^\circ$. Rotating each servo in the opposite direction gives the ability to rotate the FSS.

5 Pneumatics

As the pneumatic systems produce thrust and are responsible for the floatation, they are the fundamental core elements of any FSS. In the case of MyDAS, the main elements are a pressurized air tank, a pressure regulator, air bearings and thrusters. A preliminary Bill of Materials (BoM) for the pneumatic parts is listed in the appendix in Table 8.1.

5.1 Compressed Air Supply

Like the older generations, this Floating Spacecraft Simulator uses compressed air to feed the air bearings and the thrusters. The use of Compressed CO₂ cartridges was examined, but several properties are unknown. Experimentally testing these would be out of the scope for this thesis. The ease of refilling air tanks compared to CO₂ cartridges further motivated the use of air among other reasons. Different compressed air tanks are considered. The volume of the air tanks ranges from 9 ci (0.15l) to 15 ci (0.25l) and the pressure ranges from 3000 psi (207 bar) to 4500 psi (310 bar). Most of the air tanks come from the paintball or airsoft sector, since those industries provide a standard .825x14 male thread and they come in portable sizes. In addition to that, they all have a pressure regulator that comes with them. These internal pressure regulators save space, which is important to keep the overall size of the simulator small. The shape and size, which mainly depends on the volume of air inside it, plays a major role in the design of this FSS, as the air tank with its pressure regulators is the largest component. Table 5.1 shows the three air tanks that made it to further consideration.

Name/Vendor	Pressure in psi (bar)	Volume in cubic inch (l)
Tippmann	3000 (207)	9 (0.15)
Ninja	3000 (207)	13 (0.21)
First Strike	4500 (310)	15 (0.25)

Table 5.1: The final three air tanks for consideration [19], [20], [21].

While all air tanks in this category use an acceptable amount of space, they are shaped thin and long, making the length a problematic factor. The length of the air tanks dominates the overall construction and contributes to instability. Since the Tippmann air tank is the shortest of them, it is the one used for the preliminary design of MyDAS.

Nonetheless, a generally wider, but shorter shape would be desirable. The Tippmann air tank comes with a pressure regulator that reduces the pressure from 3000 psi (207 bar) down to 850 psi (59 bar). After that, another pressure regulator decreases air pressure to 60 psi (4.1 bar). From that point on, the air is distributed to the thrusters and the floatation system. Figure 5.1 shows the pneumatic diagram of MyDAS as planned. All mentioned pressures are gauge pressures, i.e. not including atmospheric pressure.

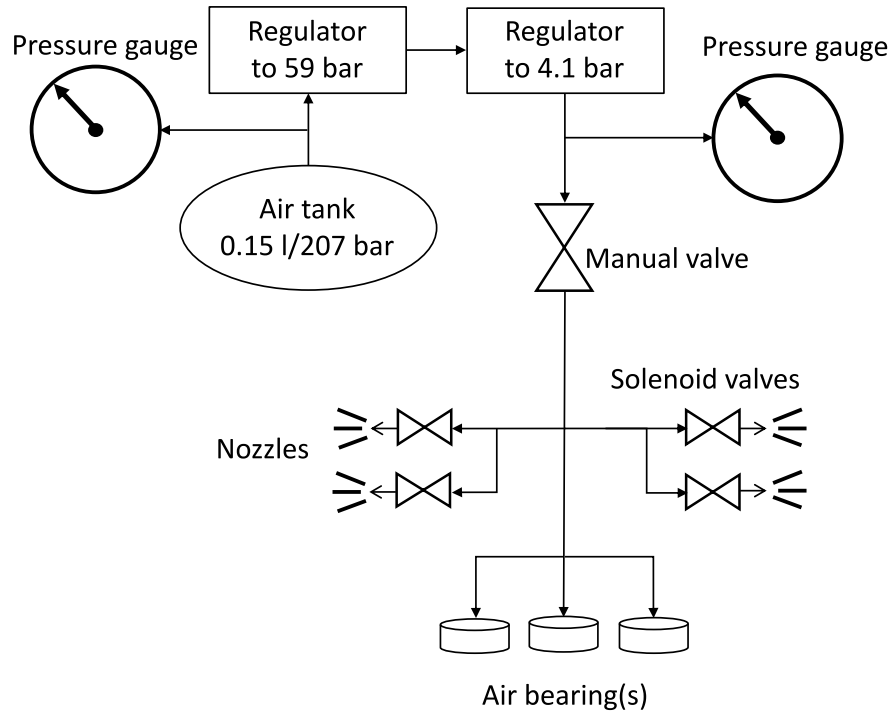


Figure 5.1: A schematic diagram showing the airflow for the pneumatics of MyDAS.

A manual valve, directly after the second pressure regulator, opens or closes the air supply for the whole pneumatic system. Instead of an electrically operated valve, a manual valve is chosen to reduce costs, space and complexity. More electronic parts, wiring, programming would be necessary to cover this ability without a manual valve.

5.2 Air Bearings

Two main design proposals are made for the floatation of the device. Either three 25 mm flat round air bearings or a single, but larger flat round air bearing can be used, all by the company of New Way[®] Air Bearings. Sizes that are under consideration were 50 mm, 65 mm and 80 mm. Figure 5.2 shows an example for an air bearing that could be used for Floating Spacecraft Simulators.

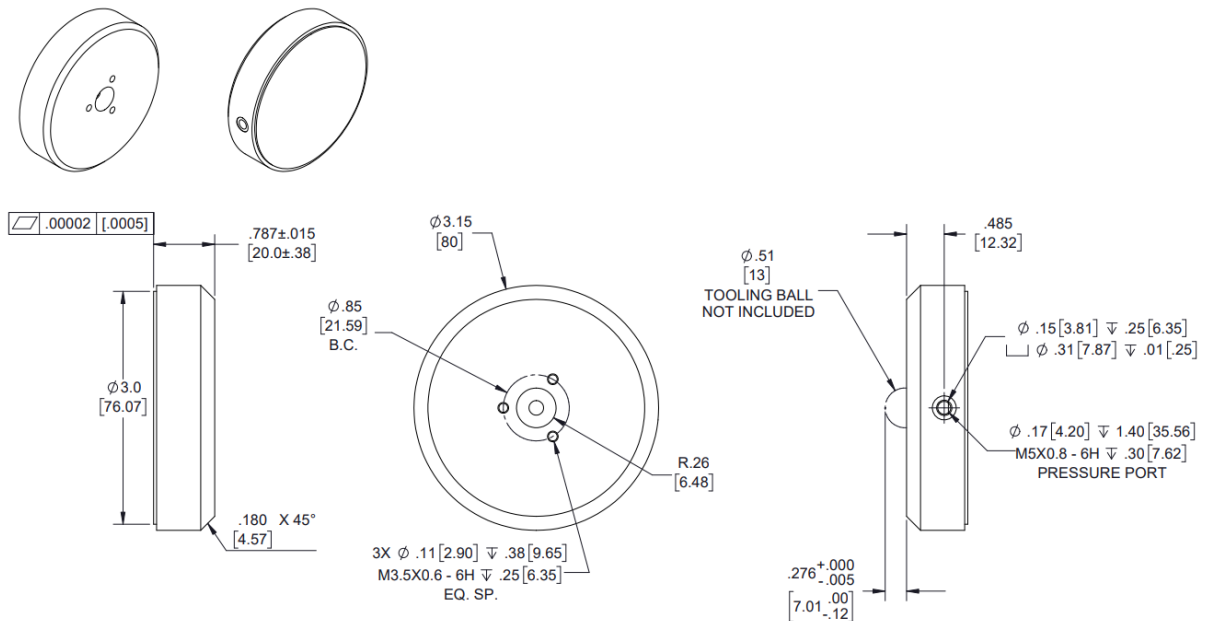


Figure 5.2: A technical drawing of an 80 mm flat round air bearing [22].

The design with three small air bearings is the one that was used in some of the older designs at NPS. A ball mounting screw ensures that the weight of the device pushes the bearing down perfectly centered. With three of these, the standing of the simulator is well defined and stable. If the center of gravity (projected to the ground) is the same distance away from every air bearing, the weight is evenly distributed across all three bearings. If the center of gravity is offset from this point, the load is unevenly distributed. This results in bigger or smaller air gaps between the bearing and the ground. From figure 5.3, it can be derived, that for the 25 mm air bearing, at around 30 N of load, even great deviations of load result in microns of lift deviation.

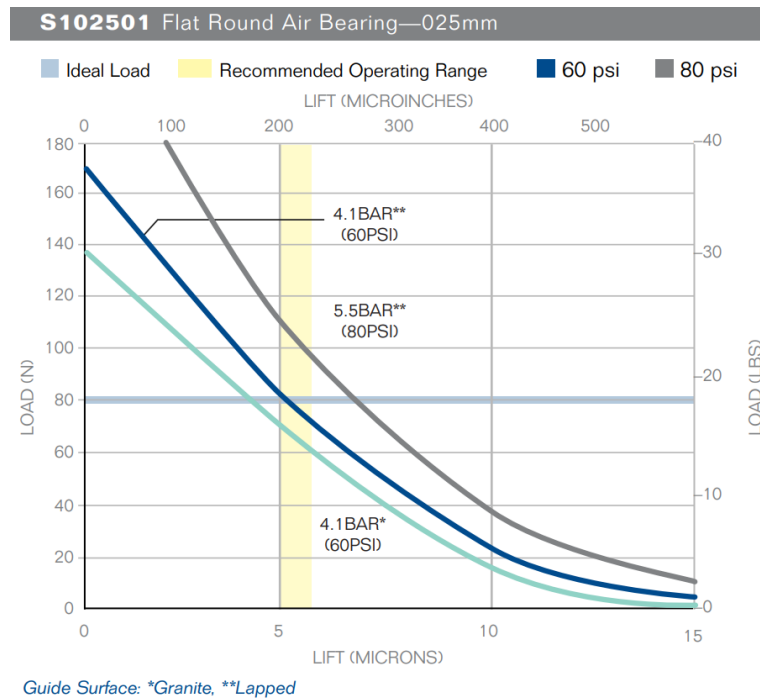


Figure 5.3: Lift versus load curve for the 25 mm flat round air bearing [23].

This small change in lift compared to the dimensions of the FSS is negligible. Furthermore, the lift does not affect the friction of the air bearing and therefore, the configuration of three small air bearings can be seen as stable and immune to the location of the center of gravity. Two main downsides of this configuration are an increased tubing effort, as well as a bigger footprint. Especially the size of the footprint is a property that is ought to be decreased. By using only one air bearing, the limiting factor for footprint is not the air bearings anymore, but all the other components above the air bearing. The major disadvantage of using one air bearing only is the fact that the structure above it must be mounted via a rigid connection, meaning that the ball mounting screw is not an option, since that cannot convey any torque and anything above it could not stand. A rigid connection, however, could create a pitch moment, pushing the air bearing asymmetrically to the ground, risking contact between the ground and the edge of the air bearing. The pitch moment increases with decreasing size of the air bearing and it increases as the center of gravity (projected to the ground) is further away from the center of the air bearing.

All in all, choosing the right air bearing configuration is a compromise between the size of the footprint, stability, simplicity and air consumption. For the single configuration, larger size means more stability but higher air consumption. Furthermore, the ideal load is far more off the real load for larger air bearings. Three small air bearings provide the greatest stability, but are the most complex build and require the greatest footprint. The total weight of MyDAS is estimated to be less than 5 kg. In comparison to the older generations of FSS, this is much lighter. However, air bearings are generally designed to carry higher loads. Table 5.2 shows the ideal loads for each size of flat round air bearings as given by the manufacturer. The load is sometimes given as a weight and sometimes as a force. Correctly, it should be indicated as a force, but if given as a weight, Earth's surface gravity of 9.81 m/s^2 is assumed.

\varnothing in mm	Ideal load in lbs (kg)
25	18 (8.2)
50	80 (36)
65	150 (68)
80	250 (113)

Table 5.2: Air bearings of different diameters with their corresponding ideal load [24].

It must be mentioned that for the option of using three 25 mm air bearings, the ideal load will have to be multiplied by 3, resulting in about 24 kg. That would still be the lightest ideal load, compared to the options using only a single, but larger air bearing.

5.3 Floating Duration

Since the source of air for the air bearings and the thrusters comes from a closed air tank, the air supply is not endless. To estimate how long the spacecraft simulator can float (without activating thrusters), two main factors have to be taken into account. One is the the amount of air that is available and the other is the outflow, i.e. how much air is used per time. Without the use of measuring instruments, both factors can only be estimated roughly. An estimate for the mass of air available in the air tank can be achieved by multiplying the air density inside the tank by the volume of the tank. These values are shown in Table 5.3. For reading the density off a graph, an air temperature of 27°C was assumed.

$\rho_{\text{air,high}}$	215 kg/m ³ [25]
V_{airtank}	147 cm ³ [19]
ϑ_{air}	27 °C
m_{air}	31.6 g

Table 5.3: Values for determination of mass of air inside air tank.

The outflow is harder to calculate, as the air flow through the bearings can only be experimentally determined to get an accurate value. However, this thesis only covers the conceptual design of MyDAS, thus, the manufacturer's specifications are used. The "no load flow" at 4.1 bar for each of the considered air bearings is shown in Table 5.4 in the second column [24]. In addition to that, the potential floating time is calculated under the assumption that the entire air from the air tank can be used.

\varnothing in mm	Flow in SCFH [24]	Flow in g/min	Time in min
25	1.3 - 1.6	0.8 - 0.9	42 - 34
50	2 - 3.2	1.2 - 1.8	17 - 27
65	2.2 - 3.5	1.3 - 2.0	16 - 25
80	5 - 7.5	2.9 - 4.3	7 - 11

Table 5.4: Air flow and floating time for each air bearing under no load at 4.1 bar.

The flow in Standard Cubic Feet per Hour (SCFH) is given by the manufacturer, while the flow in g/min was calculated by multiplying with the air density at the conditions used for SCFH, which are 101.325 kPa and 288.706 K. At these conditions, the density of air is $\rho_{\text{air,low}} = 1.222 \text{ kg/m}^3$ [26]. After converting cubic feet to liters, hours to minutes and multiplying the density with the volumetric flow, one finds out that one SCFH is roughly equivalent to 0.58 g/min.

This allows to convert the volumetric flow into a mass flow. By dividing the available mass by the mass consumption flow, the potential floating time can be calculated. Table 5.4 lists these times for each bearing in in column 4, but for the 25 mm bearing, the time must be divided by three because three of them would be used at a time. Nonetheless, these times are just rough estimates. Experiments will have to be done to understand what the airflow under the load of MyDAS will be. Additionally, as the real load is to be expected much less than the ideal load, the air bearings might also work under lower pressure, decreasing air flow and thus increasing floating time.

5.4 Thrusters

Each thruster consists of two subcomponents. One is an electrically operated solenoid valve, and the other is the thruster nozzle. The nozzle used for MyDAS is a custom built laval-nozzle by the SRL and is depicted in Figure 5.4, where it is mounted onto the solenoid valve. The air comes from the valve on the left and exits through the orifice, which is visible on the right. The solenoid valves are either fully open or fully closed and do not allow any states in between.

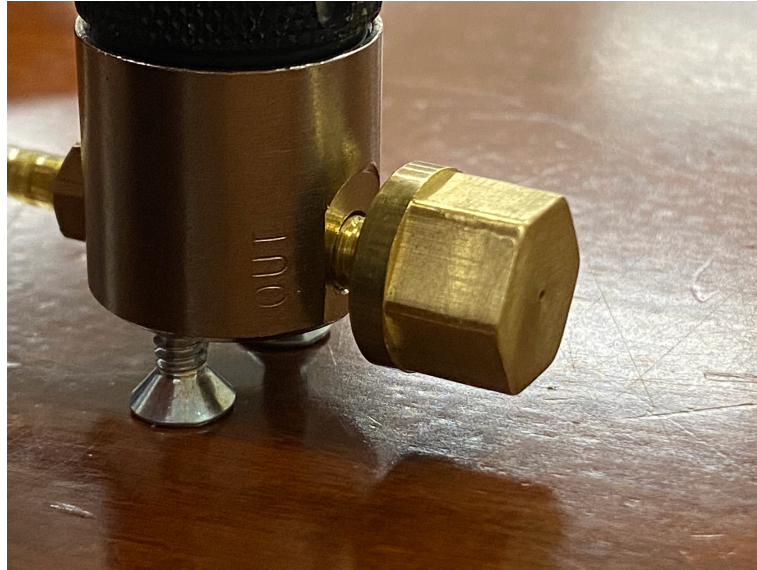


Figure 5.4: Laval nozzle used for MyDAS, mounted onto the solenoid valve.

SRL's third generation of planar FSS had used the same solenoid valves and nozzles. At 6.9 bar, each thruster produced roughly 0.16 N of thrust [27]. By assuming linear thrust and input pressure correlation, for use at 4.1 bar, approximately 0.1 N of thrust could be achieved.

6 Electronics

The electronic parts are responsible for giving the Floating Spacecraft Simulator its maneuverability. As discussed in previous chapters, different propulsion methods are possible, but all of them are controlled electronically, since the actuators are controlled by GNC algorithm, which runs electronically. To achieve all of this, an on-board power supply, a processing unit, voltage converters, solenoid valves and wires are necessary. Depending on the propulsion mechanism, servos are additionally used. A preliminary BoM for the electronic parts is listed in the appendix in Table 8.3.

6.1 Power Supply and Distribution

As the Floating Spacecraft Simulator has almost no friction in the horizontal plane, having a cable connected to the device would inevitably influence the dynamics of the FSS, as a cable has a certain weight and stiffness. Therefore, an on-board electronic power supply is used. Because the on-board computer is supplied at 5 V, but the solenoid valves work at 12 V, either two separate power supplies or at least one voltage converter have to be present. For MyDAS, it was decided to use only one battery with voltage converters to cover all supply voltages. This layout is chosen for minimal space and mass requirements, as an additional battery would use much more of both, compared to a voltage converter. Generally, a wide variety of batteries is eligible, but the smallest and lightest battery is preferred. Because the preferred batteries deliver around 11.1 V, it is necessary to use one voltage converter for the on-board computer and one for the solenoid valves. After the battery, a Y-harness splits the power cable into two circuits. The first pair of cables is connected to a voltage converter that decreases the voltage from 11.1 V to 5 V. This pair of cables powers the on-board computer directly, as well as the servos and an optional Inertial Measurement Unit (IMU). The second pair of cables runs to a voltage converter which boosts the voltage to 12 V for the solenoids.

To switch the solenoids on and off, a relay for each solenoid is necessary. After the 12 V converter, the power cables split up again, entering the relays. Depending on the propulsion configuration, the cables split up into two or four, and either a two channel relay or a four channel relay is used. The relays operate at 5 V and can be controlled directly by the on-board computer. Figure 6.1 shows in a schematic manner how the battery supplies power to the on-board computer, the solenoids, as well two relays, a servo motor and an IMU.

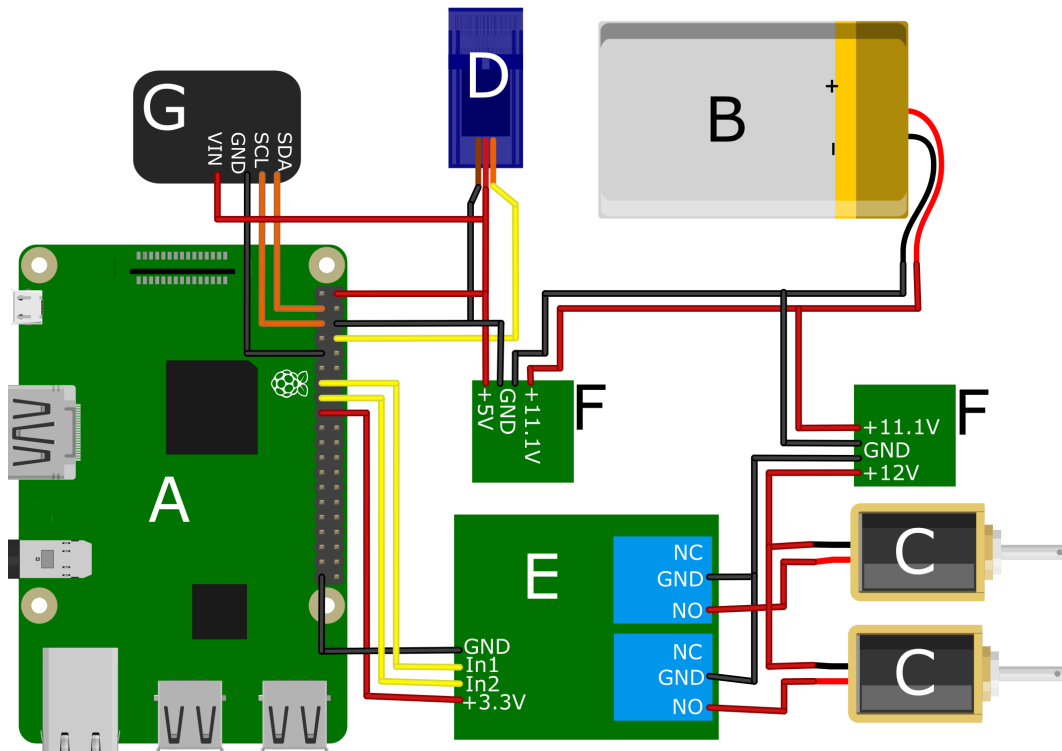


Figure 6.1: A schematic diagram of the wiring for MyDAS.

On the left, the on-board computer (A), in this case a Raspberry Pi 3, can be seen with its GPIOs. In the top right is the 11.1 V battery (B), and on the right bottom there are two solenoid valves (C). In the center top, there is, for simplification reasons, only one servo (D). The green part in the bottom with two blue boxes represents a two-channel relay (E) and the two smaller green parts represent the voltage converters (F) to 5 V and 12 V. To the left of the servo, seen in black is a six DoF IMU (G) that draws its power from the 5 V voltage converter and sends data via two cables to the on-board computer.

6.2 Electronic Parts

The central power supply provides power to a number of parts. In the following, these are explained in specific.

6.2.1 On-Board Computer

The control signals for the propulsion systems must come from a processing unit that is mounted on the simulator. Even though remote control solutions could be realized, it is assumed to be the simplest way to use one centralized on-board computer to gather position and orientation data, process these by a GNC algorithm to give orders to the actuators. Cheap and widely known mini-computers are Raspberry Pi, Arduino and Jetson Nano. For reasons of availability, a Raspberry Pi was chosen, but there is no general disqualification for either of these three. As the Raspberry Pi is primarily designed to be powered by micro-USB or USB-C, depending on the generation, it is also possible to power by GPIO pins. For reasons of wiring, the latter option is chosen for MyDAS.

6.2.2 Solenoid Valves

In order to produce thrust, pressurized air is accelerated through a laval nozzle, creating a reaction force in the opposite direction, as explained in the chapter 2. To control the thrusters, a two way normally closed solenoid valve by the manufacturer GemsTM Sensors & Controls is used. When the solenoid is powered, the valve opens and air flows through it, creating thrust. When it is not powered, it is closed and no air flows. It uses an input voltage of 12 V and consumes 0.65 W of power. Its Maximum Operating Pressure Difference (MOPD) is 125 psi (8.6 bar).

6.2.3 Servos

In section 2.2, one propulsion configuration that includes servo motors is presented. For this configuration, the servos define the direction of the thrust, making their current rotational state of great interest. Hence, the decision was made to use 180° servos instead of continuous servos, as the continuous servos lose track of their exact angular position over time. Like for all other components, the smallest off-the-shelf solution is preferred. For that reason, a 9 g micro servo is chosen. It draws its power from the battery via the 5 V converter and gets control from the on-board computer.

6.2.4 Sensors

To let the FSS know its position and attitude, which is essential for any GNC algorithm, one option is to use an indoor GPS-Sensor. Because it was used in experimental builds at the SRL, HTC's VIVE tracking system is considered for MyDAS. It consists of one tracker that is to be mounted onto the FSS and two static base stations which localize the position and orientation of the tracker. The tracker is charged via a USB-cable and has its own battery. For the hardware architecture, the only thing that needs to be regarded when including this system is a single screw mount for the tracker. Figure 6.2 shows the setup for HTC's VIVE tracking system at the SRL. On the left and on the right are two base stations, capturing the motion of the tracker, which is mounted on top of an experimental FSS, seen in the middle.

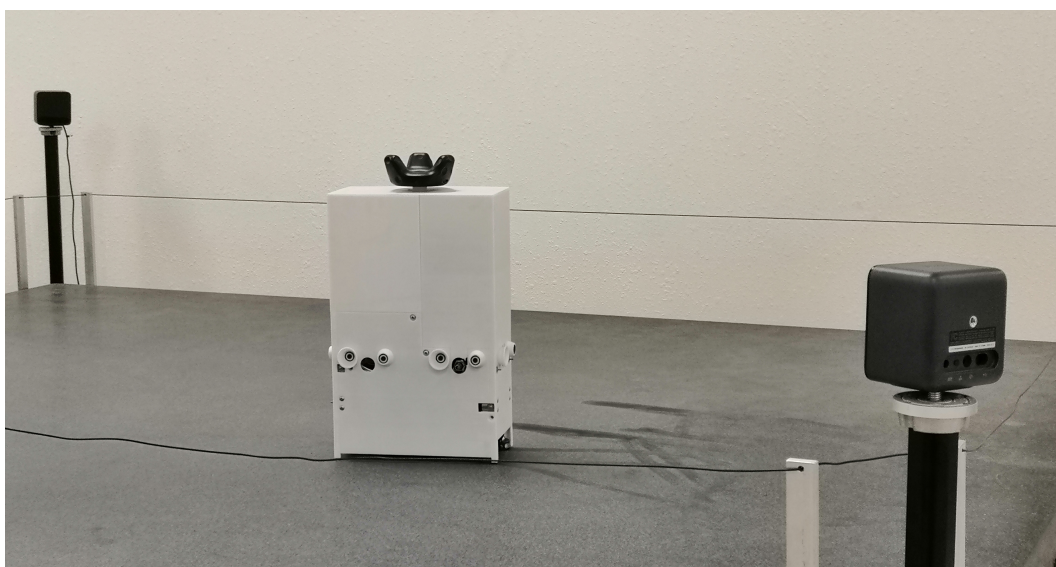


Figure 6.2: An exemplary setup for the VIVE tracking system.

Another possibility is to use static cameras that track small markers on the FSS. This principle with a commercial solution called VICON was utilized in [15]. Mounting small markers on the device requires almost no additional designing effort for the FSS. However, setting up an optical tracking system like VICON requires more effort around the testbed compared to the VIVE tracker. Therefore, MyDAS is recommended to be used with HTC VIVE, but it shall also be compatible to be used with systems like VICON.

Determining speed and acceleration will be done in either of two ways. Firstly, the positioning data of the tracking system could be derived once for speed and twice for acceleration. Secondly, the acceleration could be taken from an IMU and the speed could be obtained by integrating this acceleration. For this reason, MyDAS will be equipped with an IMU. If, the IMU is not chosen to provide the acceleration and speed data, it can still be used for validation, as done in [10].

7 Design Work

In order to gain a fully functional Floating Spacecraft Simulator, all core elements must be held together by a frame. The frame of the older generations of FSS at the SRL is of cuboid shape and it contains all components within its bounding box. The idea behind it was to create a defined volume and then packing all necessary parts inside it. However, this approach wastes a lot of space. For MyDAS, a different approach is planned, creating only frame structure where it is needed. All parts of the frame are designed to be 3D-printed. A preliminary BoM for the frame is listed in the appendix in Table 8.2.

7.1 3D Sketching

First, all the essential components are either measured and modeled in a 3D software or a CAD-file is downloaded from the manufacturer. Second, all parts for which the positioning and orientation directly affects the maneuverability are put in place. In particular, this applies to the floatation system and the propulsion system, i.e. the air bearings, thrusters and for one configuration the servos are put into place. Third, for all supportive components, solutions are figured out on where and how to put them in a manner that keeps the design as small as possible, but still stable. This step regards the air tank with its pressure regulators, the on-board computer, the battery and miscellaneous parts. While finding spaces for these supportive components, the position of the floatation and propulsion objects is adapted, creating an iterative loop. An open-source 3D software called *Blender* is used to perform steps one to three. Figure 7.1 shows a digital mock-up some of the most important components as they were put in empty space, visualized with Blender. In particular, the air tank, air bearings, servos, thrusters and the air regulators with pressure gauge are included.



Figure 7.1: A render of the most important components in place, but without a frame.

7.2 Conceptual Parametric Modeling

In a fourth step, after finding ideal positions for all parts, the parametric modeling of the frame itself is taken on with Autodesk's CAD software *Fusion 360*. *Fusion 360* can be obtained for free for hobby or educational users, which makes it destined to be used in an open-source hardware project. For the parametric modeling, a fixation for each component is considered. The air tank has no fixations, so a simple round bottle container is designed around it, which it can stand in. On the bottom of that container, counterbore holes are incorporated to screw the container onto one of the bigger air bearings. The 50 mm, 65 mm and 80 mm air bearings have threaded holes. All of these bearings have the holes in the same place, making the bottle container universally mountable on all the mentioned sizes of air bearings. For the 25 mm air bearing, a platform with three arms is constructed. The platform incorporates the same holes as the bigger air bearings, enabling the bottle container to be screwed onto this platform. Each of the three arms has a 13 mm half dome facing down. This half dome fits into the spherical hole of the 25 mm air bearings, fixating it in all side directions. When the platform is lifted up, however, the half domes fall out of the 25 mm air bearings, as it is not fixated in the vertical axis. For operational use, this does not matter.

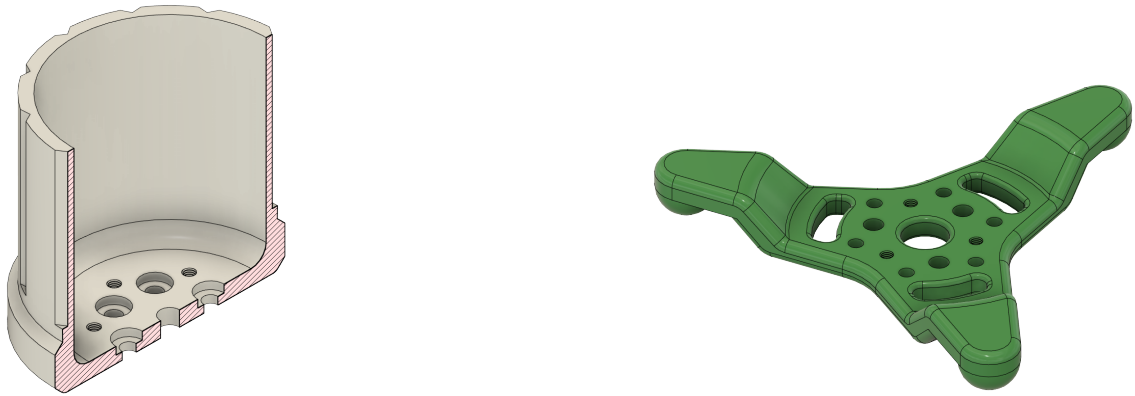


Figure 7.2: Illustration of the bottle container and the platform.

Figure 7.2 shows the cross section of the bottle container (left) as well as the three-armed platform (right) in Fusion 360. To hold the propulsion systems, a ring around the bottle container is designed. This ring will be put around the bottle container from the top, constraining it in all side directions, while being pulled down by gravity. To fix it on its rotational axis, the bottle container has grooves and the ring around it has ridges, fitting in these grooves. For the 4-thrusters-configuration, four arms at 90° spacing are on this ring. At the end of each arm is a small platform with several holes in it. These can be used to screw the solenoid valves on them, facing in different directions. This allows to choose between the cross or the parallel configuration. The vector configuration has only two arms on the ring. Each arm has mounting holes for the servos to be aligned and screwed onto the propulsion ring. To mount the solenoid valves onto the servos, a small, custom designed adapter will be used. Figure 7.3 depicts the ring for the parallel or diamond thruster configuration on the left and the servo configuration on the right.

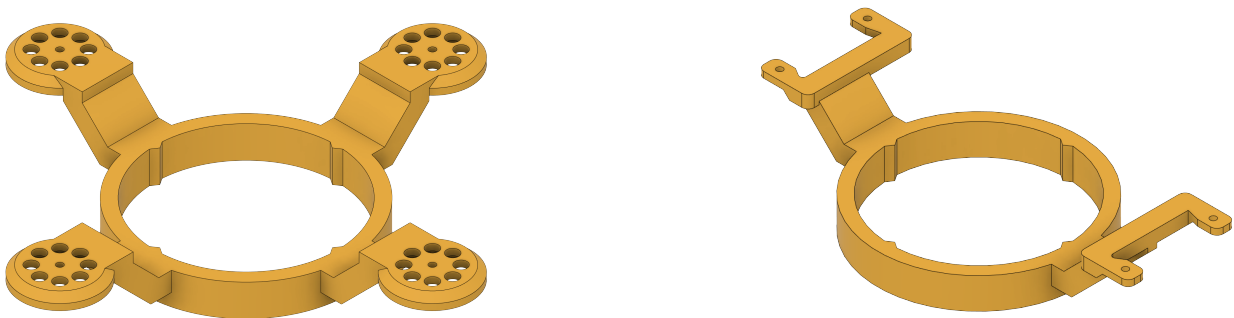


Figure 7.3: Illustration of thruster and servo mounting rings.

For all the electronic parts, further rings are designed. Each ring has the same ridges to fit on the bottle container, but also has custom arms for mounting different objects, like the battery or the on-board computer.

7.3 Conceptual Assembly

The fifth and last step is to put together the wiring and tubing, but this act should be tackled when the rest of the assembly has been physically completed. Therefore, this is due in future work and is not investigated in this paper. This design approach has two main advantages to previous FSS. It uses much less space and mass for the frame, keeping the device as small as possible. Additionally, with the features described above, swapping out the air bearings or changing the thruster configuration requires minimal effort. Figure 7.4 shows two variants for MyDAS assembled in Fusion 360. On the left, the diamond thruster configuration together with the three air bearings configuration is combined.



Figure 7.4: Assembly of some components for two variants of MyDAS.

The view is deliberately from below to show the platform (in green) on which the bottle container (white) is screwed. On the right leg of the green platform, one air bearing is hidden to show the half dome that fits into the top of the air bearing. The yellow ring with its four hands to screw the solenoids is also shown, as it is rotationally fixed using the grooves from the bottle container. Dominating the assembly by its size in comparison to everything else, the black Tippmann air tank is shown in both depictions. On the right hand side, the bottle container and air tank remain the same. However, instead of the three-armed platform for three air bearings, the bottle container is mounted directly on top of the 65 mm flat round air bearing. Instead of the four-armed ring, the two-armed ring for the servos is shown on the right picture. Mounted to the ring is the servo plus servo arm, servo adapter and solenoid inclusive nozzle for each side. All propulsion configurations can be combined with all air bearing configurations, creating maximum flexibility and adaptivity.

8 Conclusions

After having started the project of MyDAS, a number of conclusions are drawn. Yet, a lot of work is ahead of launching this Floating Spacecraft Simulator to the public. The following two sections give an overview of what has been achieved and what is desired to be achieved.

8.1 Summary

A design proposal for a new Floating Spacecraft Simulator is made, with the name of MyDAS. It is targeted at researchers, institutions, companies or hobby users who could not have afforded to work on FSS before, either out of lack of funding or increased effort to design, build and run a FSS and its associated test-bed. The new design primarily focuses on a smaller size compared to previous FSS. Hence, smaller and accordingly cheaper test-beds are necessary to conduct tests with the simulator. Additionally, the design keeps the number of parts to a minimum, promoting simplicity. Functional parts, for instance the air bearings or on-board computer, are picked off-the-shelf. All parts are checked for compatibility while operational limits of pressure, current or voltage are incorporated. For pneumatic or electric connections, standardized solutions are chosen, giving the target group the opportunity to exchange parts, while still being able to connect them to the system. Some of the frame design has been done, with options to change the propulsion and floatation method. The frame for MyDAS will be 3D-printed, with the CAD drawings being freely accessible. Having the standardized, open-source and adaptive design gives future users not only the ability to purchase and assemble the device from scratch, but also allows for improvement and individualization. In all aspects, pricing is highly regarded in order to motivate the target group to use MyDAS for their research.

8.2 Future Work

As the device of MyDAS has only been conceptually designed, but not yet built, its physical assembly has yet to be done. Before that, the final frame needs to be designed and manufactured. Efficient tubing and wiring is due for future work as well, as this is hard to plan on paper. After testing all components by themselves for functionality, the complete system will have to be assembled and tested again for functionality. Mechanical properties like mass and center of gravity should be determined. Additionally, the equations of motion for each propulsion configuration should be explicitly identified. Regarding the air bearings, experimental testing will need to be done to find out at what pressure the air bearings work well, while consuming as little air as possible. In that turn, it is also recommended to test all air bearing configurations for stability, air consumption and practicality. By the current design, the thrusters use the same input pressure as the air bearings. Test runs will need to be done to verify that the thrusters work as desired when using the same pressure as the air bearings. Lastly, a closed-loop control must be integrated to enable GNC command. After all these steps, MyDAS will be ready to be used to experimentally test GNC algorithms.

References

- [1] NASA. *NASA Technology Roadmaps: TA 4: Robotics and Autonomous Systems*. 2015. URL: https://www.nasa.gov/sites/default/files/atoms/files/2015_nasa_technology_roadmaps_ta_4_robotics_and_autonomous_systems_final.pdf (visited on 03/15/2022).
- [2] Qi Li, Jianping Yuan, and Huan Wang. “Sliding mode control for autonomous spacecraft rendezvous with collision avoidance”. In: *Acta Astronautica* 151 (2018), pp. 743–751. ISSN: 0094-5765. DOI: 10.1016/j.actaastro.2018.07.006.
- [3] Marco B. Quadrelli et al. “Guidance, Navigation, and Control Technology Assessment for Future Planetary Science Missions”. In: *Journal of Guidance, Control, and Dynamics* 38.7 (2015), pp. 1165–1186. DOI: 10.2514/1.G000525.
- [4] Jason Hall and Marcello Romano. “Autonomous Proximity Operations of Small Satellites with Minimum Numbers of Actuators”. In: *AIAA/USU Conference on Small Satellites*, pp. 1–14.
- [5] New Way Air Bearings. *Air Bearing Application and Design Guide*. Pennsylvania, 2021. URL: <https://www.newwayairbearings.com/wp-content/uploads/2021/07/NWAB-Design-and-App-Guide-ver-12-2021.pdf> (visited on 03/10/2022).
- [6] Akshay Reddy Tummala and Atri Dutta. “An Overview of Cube-Satellite Propulsion Technologies and Trends”. In: *Aerospace* 4.4 (2017). ISSN: 2226-4310. DOI: 10.3390/aerospace4040058.
- [7] Claudio Lugini and Marcello Romano. “A ballistic-pendulum test stand to characterize small cold-gas thruster nozzles”. In: *Acta Astronautica* 64.5 (2009), pp. 615–625. ISSN: 0094-5765. DOI: 10.1016/j.actaastro.2008.11.001.
- [8] Jana L. Schwartz, Mason A. Peck, and Christopher D. Hall. “Historical Review of Air-Bearing Spacecraft Simulators”. In: *Journal of Guidance, Control, and Dynamics* 26.4 (2003), pp. 513–522. DOI: 10.2514/2.5085.
- [9] Fred Hadaegh and Kirk Munsell. *Formation Control Testbed*. 21/08/2012. URL: https://dst.jpl.nasa.gov/test_beds/index.htm (visited on 03/20/2022).
- [10] Jonathan D. Wapman et al. “Jet Propulsion Laboratory Small Satellite Dynamics Testbed Planar Air-Bearing Propulsion System Characterization”. In: *Journal of Spacecraft and Rockets* 58.4 (2021), pp. 954–971. DOI: 10.2514/1.A34857.

-
- [11] S. Kwok-Choon et al. “Design, Fabrication, and Preliminary Testing of Air-Bearing Test Vehicles for the Study of Autonomous Satellite Maneuvers”. In: *31st Florida Conference on Recent Advances in Robotics*. 2018.
- [12] Tomasz Rybus et al. “New planar air-bearing microgravity simulator for verification of space robotics numerical simulations and control algorithms”. In: *12th ESA Symposium on Advanced Space Technologies in Robotics and Automation*. 2013, p. 8.
- [13] Giovanni Palmerini, Marco Sabatini, and Paolo Gasbarri. “Analysis and tests of visual based techniques for orbital rendezvous operations”. In: *2013 IEEE Aerospace Conference*. 2013, pp. 1–14. DOI: 10.1109/AERO.2013.6497417.
- [14] Marco Sabatini, Giovanni B. Palmerini, and Paolo Gasbarri. “A testbed for visual based navigation and control during space rendezvous operations”. In: *Acta Astronautica* 117 (2015), pp. 184–196. ISSN: 0094-5765. DOI: 10.1016/j.actaastro.2015.07.026.
- [15] Richard Zappulla et al. “Floating Spacecraft Simulator Test Bed for the Experimental Testing of Autonomous Guidance, Navigation, & Control of Spacecraft Proximity Maneuvers and Operations”. In: *AIAA/AAS Astrodynamics Specialist Conference*. DOI: 10.2514/6.2016-5268.
- [16] Jason Hall and Marcello Romano. “Laboratory Experimentation of Guidance and Control of Spacecraft During On-Orbit Proximity Maneuvers”. In: *Mechatronic Systems Simulation Modeling and Control*, pp. 187–222. DOI: 10.5772/9132.
- [17] Markus Wilde, Casey Clark, and Marcello Romano. “Historical survey of kinematic and dynamic spacecraft simulators for laboratory experimentation of on-orbit proximity maneuvers”. In: *Progress in Aerospace Sciences* 110 (2019), p. 100552. ISSN: 0376-0421. DOI: 10.1016/j.paerosci.2019.100552.
- [18] Tomasz Rybus and Karol Seweryn. “Planar air-bearing microgravity simulators: Review of applications, existing solutions and design parameters”. In: *Acta Astronautica* 120 (2016), pp. 239–259. ISSN: 0094-5765. DOI: 10.1016/j.actaastro.2015.12.018.
- [19] ANS Gear. *TIPPMANN 9/3000 FLAT BOTTOM ALUMINUM COMPRESSED AIR TANK*. 2022. URL: https://www.ansgear.com/Tippmann_9_3000_Flat_Bottom_Compressed_Air_Tank_p/tippmantank93000.htm (visited on 03/25/2022).
- [20] Paintball Online. : *Ninja Compressed Air Tank - Aluminum Flat Bottom - 13/3000*. 2022. URL: <https://paintball-online.com/ninja-compressed-air-tank-aluminum-flat-bottom-13-3000/> (visited on 03/25/2022).
- [21] Modern Combat Sports. *FIRST STRIKE 15CI 4500PSI CARBON FIBER HERO 2 HPA HALF PINT TANK*. 2022. URL: <https://mcsus.com/products/15ci-4500psi-carbon-fiber> (visited on 03/25/2022).

-
- [22] New Way Air Bearings. *80mm FLAT ROUND AIR BEARING*. 2019. URL: <https://www.newwayairbearings.com/wp-content/uploads/2017/07/S108001-C.pdf> (visited on 03/15/2022).
- [23] New Way Air Bearings. *Air Bearing Flat Round 25mm Curve Lift-Load*. URL: https://www.newwayairbearings.com/wp-content/uploads/2017/07/air_bearing_flat_round_025mm_curve_lift-load_new_way_S102501_en.pdf (visited on 03/15/2022).
- [24] New Way Air Bearings. *Porous Media Air Bearing Solutions: Flat Round*. URL: https://www.newwayairbearings.com/wp-content/uploads/2020/01/16247464_-_NWAB_-_December_2019_-_Flat_Round_Brochure_V2.pdf (visited on 03/15/2022).
- [25] Engineering ToolBox. *Air - Density vs. Pressure and Temperatures*. 2004. URL: https://www.engineeringtoolbox.com/air-temperature-pressure-density-d_771.html (visited on 03/16/2022).
- [26] Engineering ToolBox. *Air - Density, Specific Weight and Thermal Expansion Coefficient vs-Temperature and Pressure*. 2003. URL: https://www.engineeringtoolbox.com/air-density-specific-weight-d_600.html (visited on 03/16/2022).
- [27] Markus Wilde et al. “Experimental Characterization of Inverse Dynamics Guidance in Docking with a Rotating Target”. In: *Journal of Guidance, Control, and Dynamics* 39.6 (2016), pp. 1173–1187. DOI: 10.2514/1.G001631.

Appendix

Name	Details	Price	Amount	Function
air bearing	∅ 80 mm	\$ 325.00	1	floatation
air bearing	∅ 65 mm	\$ 215.00	1	floatation
air bearing	∅ 50 mm	\$ 185.00	1	floatation
air bearing	∅ 25 mm	\$ 155.00	3	floatation
thruster nozzle	custom made	\$ 0.00	4	propulsion
solenoid valve	12 V, 125 psi	\$ 64.00	4	propulsion
Ninja air tank	13 ci/3000 psi	\$ 71.95	1	air tank
First Strike air tank	15 ci/4500 psi	\$ 224.95	1	air tank
Tippmann air tank	9 ci/3000 psi	\$ 49.95	1	air tank
Palmer air regulator	90°, 4500 psi to 60 psi	\$ 131.32	1	air flow control
pressure Gauge	160 psi range	\$ 12.07	1	air flow control
manual valve	1/8 NPT F-M	\$ 13.24	1	air flow control
air fitting thread-barb	M3 to 1/16"	\$ 3.55	3	tube connector
air fitting thread-barb	M5 to 1/16"	\$ 3.06	1	tube connector
air fitting thread-barb	10-32 to 1/16"	\$ 3.89	4	tube connector
air fitting thread-thread	1/8 NPT M-F	\$ 2.15	1	tube connector
air fitting thread-thread	1/8 NPT M-F, 90°	\$ 1.33	1	tube connector
push-to-connect	1/8 NPT to 1/8" OD	\$ 2.13	1	start of tubing
air fitting barb-barb T	1/16" tube ID	\$ 8.05	2	tubing
air fitting barb-barb X	1/16" tube ID	\$ 14.29	2	tubing
air tube 50 ft	1/8" OD, 1/16" (.066") ID	\$ 10.98	1	tubing

Table 8.1: Complete parts list for the pneumatics, including different options.

Name	Details	Price	Amount	Function
bottle container	holds the air tank	\$ 0.00	1	frame
3-arm-platform	tripod for 25 mm bearings	\$ 0.00	1	frame
4-arm-ring	attachment for thrusters	\$ 0.00	1	frame
2-arm ring	attachment for servos	\$ 0.00	1	frame
e-ring 1	attachment for computer	\$ 0.00	1	frame
e-ring 2	attachment for battery	\$ 0.00	1	frame
e-ring 3	attachment for el. parts	\$ 0.00	1	frame
screws	M3 x 0.5, $l = 6$ mm	\$ 0.06	tbd	50 and 65mm bearing
screws	M3.5 x 0.6, $l = 10$ mm	\$ 0.05	tbd	for 80mm bearing
screws	6-32, $l = 12.7$ mm	\$ 0.06	tbd	for solenoids
screws	6-32, $l = 9.5$ mm	\$ 0.11	tbd	for solenoids
screws	M2 x 0.4, $l = 8$ mm	\$ 0.09	tbd	for servos
nuts	M2 x 0.4, $l = 1.6$ mm	\$ 0.01	tbd	for servos
screw-to-expand	M3 x 0.5, $l = 4.8$ mm	\$ 0.29	tbd	for 3D-printed parts

Table 8.2: Complete parts list for basic assembly items, including different options.

Name	Details	Price	Amount	Function
on-board computer	Raspberry Pi 3 or 4	\$ 35.00	1	runs GNC algorithm
micro SD	64 GB	\$ 13.41	1	digital storage
servo	4.8 V - 6 V	\$ 5.85	2	thrust-vectoring
IMU	6 DoF, 3.3 V-5 V	\$ 6.95	1	positioning system
HTC Vive Tracker	on-board tracker	\$ 129.99	1	positioning system
Base Station	connects to tracker	\$ 114.99	2	positioning system
battery	11.1 V, 1.8 Ah, EC3 male	\$ 11.99	1	power supply
voltage converter	3 V-30 V \rightarrow 12 V, 2 A	\$ 24.95	1	power for solenoids
voltage converter	2.8 V-22 V \rightarrow 5 V, 4 A	\$ 19.95	1	power for computer
voltage converter	2.7 V-11.8 V \rightarrow 3.3 V, 1.5 A	\$ 11.95	1	power for servos
PCB	4 cm x 6 cm	\$2.50	1	wiring platform
relay	5 V, 4 channel	\$ 5.01	1	thruster control
relay	5 V, 2 channel	\$ 5.01	1	thruster control
jumper cables	3" M-M	\$ 2.85	tbd	general wiring
jumper cables	3" M-F	\$ 2.85	tbd	general wiring
jumper cables	3" F-F	\$ 2.85	tbd	general wiring
cable splitter	Y-harness EC3	\$ 11.99	1	general wiring
cable adapter	EC3 male	\$ 5.99	1	general wiring

Table 8.3: Complete parts list for the electronics, including different options.